DEUTSCHES ELEKTRONEN-SYNCHROTRON DESY

DESY 66/22
September 1966
Experimente

Photoproduction of Single Positive Pions between 1.2 and 3 GeV

by

G. Buschhorn, J. Carroll, R.D. Eandi
P. Heide, R. Hübner, W. Kern, U. Kötz,
P. Schmüser, and H.J. Skronn

Deutsches Elektronen-Synchrotron DESY, Hamburg,
and
II. Institut für Experimentalphysik der Universität
Hamburg,
Germany.

2 HAMBURG 52 · NOTKESTIEG 1

PHOTOPRODUCTION OF SINGLE POSITIVE PIONS BETWEEN 1.2 AND 3 GEV

G.Buschhorn, J.Carroll, R.D.Eandi †, P.Heide, R.Hübner, W.Kern,
U.Kötz, P.Schmüser, and H.J.Skronn

Deutsches Elektronensynchrotron DESY, Hamburg
and
II.Institut für Experimentalphysik der Universität Hamburg
Germany

Abstract

Differential cross sections for the reaction $\gamma+p\rightarrow n+\pi^+$ are presented for incident photon energies between 1.2 and 3 GeV and pion center-of-mass production angles of 15 to 50 degrees.

We have measured the production of positive pions from the reaction $\gamma+p \rightarrow n+\pi^+$ using a high resolution magnetic spectrometer equipped with scintillation counter hodoscopes (Fig. 1). The pions were produced in a liquid hydrogen target by a bremsstrahlung beam obtained from an internal target of the DESY electron synchrotron. The bremsstrahlung beam was defined by two collimators, each followed by a sweeping magnet. A gas-filled quantameter was used to measure the photon flux [1].

The spectrometer magnets were mounted on a movable platform pivoted at the target center. Synchrotron magnets (C1 and C2) bent the particles away from the photon beam and provided an angular focus in the horizontal plane at H1. By means of the quadrupole doublet (Q1 and Q2) and the bending magnets (M1 and M2) a momentum-dispersed image of H1 was formed at H2. Counter hodoscope H1 measured the production angle of the particles with an effective resolution of ± 2.5 mrad. Hodoscope H2 measured a linear combination of the particle's production angle (θ) and momentum (p). By approximately matching the acceptance window of each H2 counter to the slope ($\partial p/\partial \theta$) of the pion photoproduction kinematics, we obtained a photon energy resolution of $\pm 0.4\%$, which permitted the separation of single- from multiple-pion production processes up to our highest photon energy. To first order the resolution of this "sloped window type spectrometer" [2] is independent of target size.

The passage of a particle through the spectrometer was indicated by a coincidence between the trigger counters $S_1S_2S_3S_4$. A measurement of the time-of-flight of the particle between S_1 and S_3 with a resolution of 2 nsec (FWHM) permitted the separation of pions from protons up to our maximum pion momentum of 2.75 GeV/c. A lead-scintillator-sandwich shower counter was used to measure the positron contamination of the pion sample. This contamination was found to be negligible in all our measurements.

At each occurrence of the coincidence ($S_1S_2S_3S_4$), the trajectory information from the hodoscopes, the particle time-of-flight, and the shower counter status were recorded in the memory of a PDP-5 computer. The PDP-5 served as a buffer during

transfer of the data to magnetic tape and also provided a continuous display of the data. Cross section calculations and other data analysis were done on an IBM-7044 to which the PDP-5 was attached by a data-link.

The acceptance, $A = \int d\Omega(dp/p)$, for each pair-combination of hodoscope elements was calculated by a Monte Carlo technique which included the effects of: 1) the finite size of the hydrogen target and photon beam, 2) multiple Coulomb scattering, 3) the stops determined by magnet apertures and counter sizes, and 4) pion decay in flight. The total acceptance of the spectrometer was 0.55×10^{-4} steradian. The error for the acceptances is estimated to be less than 5%.

Cross sections have been measured at pion laboratory angles from 8 to 20 degrees in 2 degree intervals, and at ten photon energies between 1.2 and 3 GeV. For each laboratory angle and photon energy the central momentum of the spectrometer was adjusted so that the kinematic region accessible only to single pion production was approximately centered in the momentum-angle acceptance of the spectrometer. In the subsequent analysis of the data only those events falling into the kinematic region for single pion production and well away from the edge of the bremsstrahlung spectrum were used to calculate the cross sections. The cross sections presented here have been corrected for empty-target background (7%), pion decay in flight (4 - 16%), nuclear absorption (8%), ambiguous events (8%), and effects of a thick target on the shape of the bremsspectrum.

The differential cross sections, $d\sigma/d\Omega_{c.m.}$, are given in Table I as a function of incident photon energy E_γ, and center-of-mass pion production angle, $\theta_{c.m.}$. (In Table I and Figs. 2 and 3, the errors given are only those associated with counting statistics; the overall systematic errors in the cross sections are estimated to be less than 9%.) These cross sections have been averaged over angular intervals of $\Delta\theta_{c.m.} = 5^\circ$ and energy intervals ranging from $\Delta E_\gamma = 0.1$ GeV at $E_\gamma = 1.2$ GeV, to $\Delta E_\gamma = 0.15$ GeV at $E_\gamma = 3.0$ GeV. We have determined that this choice of intervals does not appreciably change the energy-angle structure of the cross sections. The energy behavior of the cross

sections at $\theta_{c.m.} = 20$, 30, and 45° is shown in Fig. 2 with some Cal Tech data of Kilner[3] and Dixon[4]. The dominant feature of these cross sections is a rapid decrease with energy. Between 1.5 and 2.0 GeV incident photon energy we observe some structure in $d\sigma/d\Omega_{c.m.}$ which might be due to the nucleon isobars of masses 1924 and 2190 MeV. The angular distributions show a fairly uniform decrease with angle at all energies above 1.7 GeV. However, at the smallest energies, 1.2 and 1.34 GeV, the angular distributions begin to turn over below $\approx 30^{\circ}$, in agreement with Kilner[3]. The intermediate energies of 1.48 and 1.62 GeV apparently represent a transition region between these two types of behavior.

In Table III and Fig. 3 the data are presented in the form of $d\sigma/dt$ as a function of $-t$ at constant E_γ. These data have been averaged over energy intervals as given above and over intervals in $-t$ ranging from $\Delta t = 0.02$ to 0.075 $(GeV/c)^2$ at $-t = 0.02$ and 1.0 $(GeV/c)^2$ respectively. At photon energies above 1.75 GeV we have fitted the data with the expression $d\sigma/dt = A \cdot \exp(Bt)$. The results of this fitting procedure are given in Table II. Although this parametrization represents the dominant behavior of the cross sections rather well, the fits obtained at some energies are poor. The deviations of the experimental points from the exponential form show no apparent systematic behavior and may be due to small systematic errors in the data. The values of B given in Table II indicate that the exponential fall-off of the cross section becomes less rapid as the incident photon energy increases. Elings et al[5] obtained $B = 3.0 \pm 0.3$ $(GeV/c)^{-2}$ from their π^+ photoproduction data which is averaged over photon energies from 3.52 to 3.88 GeV. In elastic pion-nucleon scattering, however, larger values of B (≈ 8 $(GeV/c)^{-2}$) are observed at comparable momentum transfers[6]. We also note that the values of A given in table II show an approximately exponential decrease with increasing photon energy.

We wish to acknowledge the continued interest and help received from Professors W. Jentschke and P. Stähelin. The contribution of Dr. W. Bertram during the early stages of the experiment is gratefully acknowledged. Sincere thanks go to Mr. F. Akolk for setting up the PDP system and interfaces, and to Mr. P. E. Kuhlmann for writing the necessary IBM system programs. Finally, we thank Dr. H. O. Wüster and the DESY computation center staff for their efforts, and Mr. H. Kumpfert and the synchrotron operating crew for their efficient running of the machine.

REFERENCES

† NATO Postdoctoral Fellow, on leave from University of California Lawrence Radiation Laboratory.

1) R.R. Wilson, Nucl. Instr. 1, 101, (1957). The calibration constant for the quantameter used is $(3.49\pm0.06)\times10^{18}$ MeV/Coul as measured by A. Ladage and H. Pingel, see DESY Report No. 65/12, August 1965. (unpublished)

2) Klaus G. Steffen, High Energy Beam Optics, Interscience Publishers, New York, 1965, p. 133.

3) J.R. Kilner, thesis, California Institute of Technology, 1965 (unpublished).

4) F.P. Dixon, thesis, California Institute of Technology, 1960 (unpublished).

5) V.B. Elings, K.J. Cohen, D.A. Garelick, S. Homma, R.A. Lewis, P.D. Luckey, and L.S. Osborne, Phys. Rev. Letters, 16, 474 (1966).

6) C.C. Ting, L.W. Jones, and M.L. Perl, Phys. Rev. Letters 9, 468 (1962).

D.E. Damouth, L.W. Jones, and M.L. Perl, Phys. Rev. Letters, 11, 287(1963).

C.T. Coffin, N. Dikemen, L. Ettlinger, D. Meyer, A. Saulys, K. Terwilliger, and D. Williams, Phys. Rev. Letters 15, 838 (1965).

TABLE I: Center of mass differential cross section for the reaction $\gamma+p\rightarrow n+\pi^+$ as a function of pion center of mass production angle and incident laboratory photon energy, E_γ. The cross sections are in units of microbarns per steradian.

$d\sigma/d\Omega_{c.m.}$ (μbarns/steradian)								
	Pion production angle in center of mass system.							
E_γ(GeV)	15°	20°	25°	30°	35°	40°	45°	50°
1.20	3.64±0.11	4.03±0.13	4.37±0.11	4.36±0.14	4.41±0.11	4.06±0.20		
1.34	2.93±0.10	3.58±0.11	3.77±0.09	3.75±0.12	3.55±0.09	3.37±0.13		
1.48	3.20±0.12	3.13±0.09	3.32±0.17	2.87±0.08	2.70±0.07	2.44±0.07		
1.62	3.40±0.14	2.71±0.09	2.87±0.14	2.43±0.07	2.03±0.06	1.61±0.04	1.05±0.11	
1.77	3.28±0.14	2.90±0.08	2.72±0.07	2.36±0.06	1.78±0.06	1.39±0.04	1.17±0.06	
1.98	2.98±0.15	2.87±0.07	2.47±0.06	2.04±0.05	1.64±0.06	1.19±0.03	1.00±0.03	
2.18	2.60±0.17	2.44±0.06	2.35±0.06	1.86±0.07	1.42±0.05	1.04±0.03	0.69±0.02	0.38±0.07
2.38	2.13±0.23	1.91±0.06	1.71±0.05	1.51±0.05	1.04±0.03	0.81±0.03	0.58±0.02	0.41±0.03
2.63	2.14±0.09	1.64±0.06	1.38±0.04	1.19±0.04	0.83±0.03	0.67±0.03	0.42±0.02	0.33±0.02
2.88		1.46±0.06	1.14±0.05	1.07±0.08	0.80±0.04	0.53±0.03	0.37±0.02	0.26±0.01
3.16							0.25±0.03	0.22±0.03
3.29							0.25±0.02	0.17±0.01

TABLE II. Results of least-squares fitting our $d\sigma/dt$ cross sections with the form $d\sigma/dt = A \cdot \exp(Bt)$. The total chi-squared, χ^2, and the number of degrees of freedom, D, are given for each fit.

E_γ (GeV)	$A\left(\mu b/(GeV/c)^2\right)$	$B\ \left((GeV/c)^{-2}\right)$	χ^2	D
1.78	19.10±0.45	3.32±0.11	17.8	9
1.98	16.20±0.40	3.22±0.10	9.7	9
2.18	13.70±0.31	3.31±0.08	47.1	11
2.39	9.65±0.25	2.94±0.08	32.0	12
2.63	7.56±0.19	2.86±0.07	27.7	15
2.88	5.78±0.20	2.55±0.07	20.6	14

TABLE III $d\sigma/dt$ for the reaction $\gamma+p\rightarrow n+\pi^+$ as a function of $-t$, the four-momentum transfer squared, and E_γ, the incident laboratory photon energy. The cross sections are in units of microbarns per $(GeV/c)^2$.

$-t$ $\left(\frac{GeV}{c}\right)^2$	$d\sigma/dt$ {μbarns/$(GeV/c)^2$} Incident laboratory photon energy, E_γ, in GeV.					
	1.20	1.34	1.48	1.62	1.78	1.98
0.02	29.37±1.02	21.47±1.25				
0.05	28.09±0.94	20.68±0.58	18.52±0.59	17.69±0.69	15.97±0.76	14.57±1.92
0.07	34.35±0.93	24.81±0.73	18.92±0.64	14.32±0.57	14.45±0.47	12.70±0.42
0.10	34.72±1.10	26.11±0.79	18.70±2.58	14.12±0.75	13.50±0.47	11.82±0.42
0.12	33.68±1.20	24.91±0.95	18.51±0.64	15.24±1.00	13.64±0.45	11.16±0.43
0.15	34.18±1.06	26.71±0.95	16.47±0.67	14.34±0.49	12.11±0.49	10.58±0.39
0.18	31.52±1.30	22.66±0.68	17.02±0.67	10.87±0.45	11.58±0.37	8.90±0.32
0.21		22.80±0.87	15.73±0.44	11.15±0.40	9.79±0.39	8.76±0.29
0.25		19.40±3.50	14.05±0.50	9.60±0.29	8.07±0.28	6.89±0.29
0.30			11.49±1.35	7.89±0.29	6.76±0.21	6.20±0.28
0.35				5.68±0.72	5.95±0.22	5.04±0.18
0.40					5.13±0.53	4.54±0.16
0.46						3.46±0.20
	2.18	2.39	2.63	2.88	3.23	
0.05			7.18±0.73			
0.07	9.76±0.47	7.25±0.94	6.70±0.38			
0.10	9.11±0.33	6.86±0.31	5.55±0.34			
0.12	9.75±0.32	6.20±0.28	5.68±0.28	4.61±0.36		
0.15	8.72±0.29	6.63±0.27	4.42±0.23	3.96±0.22		
0.18	7.77±0.46	5.58±0.23	4.21±0.20	3.28±0.18		
0.21	7.45±0.44	5.81±0.25	4.05±0.19	3.18±0.20		
0.25	6.84±0.26	5.36±0.24	3.93±0.18	3.17±0.17		
0.30	5.03±0.22	3.94±0.17	3.47±0.15	2.79±0.25		
0.35	4.55±0.22	3.45±0.15	2.82±0.16	3.11±1.10		
0.40	3.99±0.15	2.93±0.15	2.25±0.12	2.31±0.18		
0.46	2.86±0.11	2.52±0.12	2.35±0.12	2.05±0.12		
0.52	2.29±0.11	2.21±0.10	1.75±0.11	1.36±0.10		
0.58	1.45±0.22	1.67±0.09	1.39±0.07	1.39±0.09		
0.65		1.17±0.13	1.13±0.07	1.11±0.08		
0.71			0.97±0.07	0.95±0.05	0.75±0.12	
0.79			0.80±0.09	0.76±0.05	0.62±0.05	
0.86				0.62±0.06	0.51±0.03	
0.93				0.64±0.09	0.41±0.04	
1.00					0.35±0.05	

FIGURE CAPTIONS

Fig. 1 Plan view of experimental arrangement.

Fig. 2 Center-of-mass differential cross sections for $\gamma+p\rightarrow n+\pi^+$ as a function of incident laboratory photon energy, E_γ. ●-this experiment, O-Reference 3, □-Reference 4.

Fig. 3 $d\sigma/dt$ as a function of $-t$ (E_γ given in GeV). ●-this experiment; O-Reference 3, E_γ = 1.20 GeV and 1.30 GeV; ∇ and Δ -Reference 5. The straight lines drawn through the data points are described in the text (see also Table II).

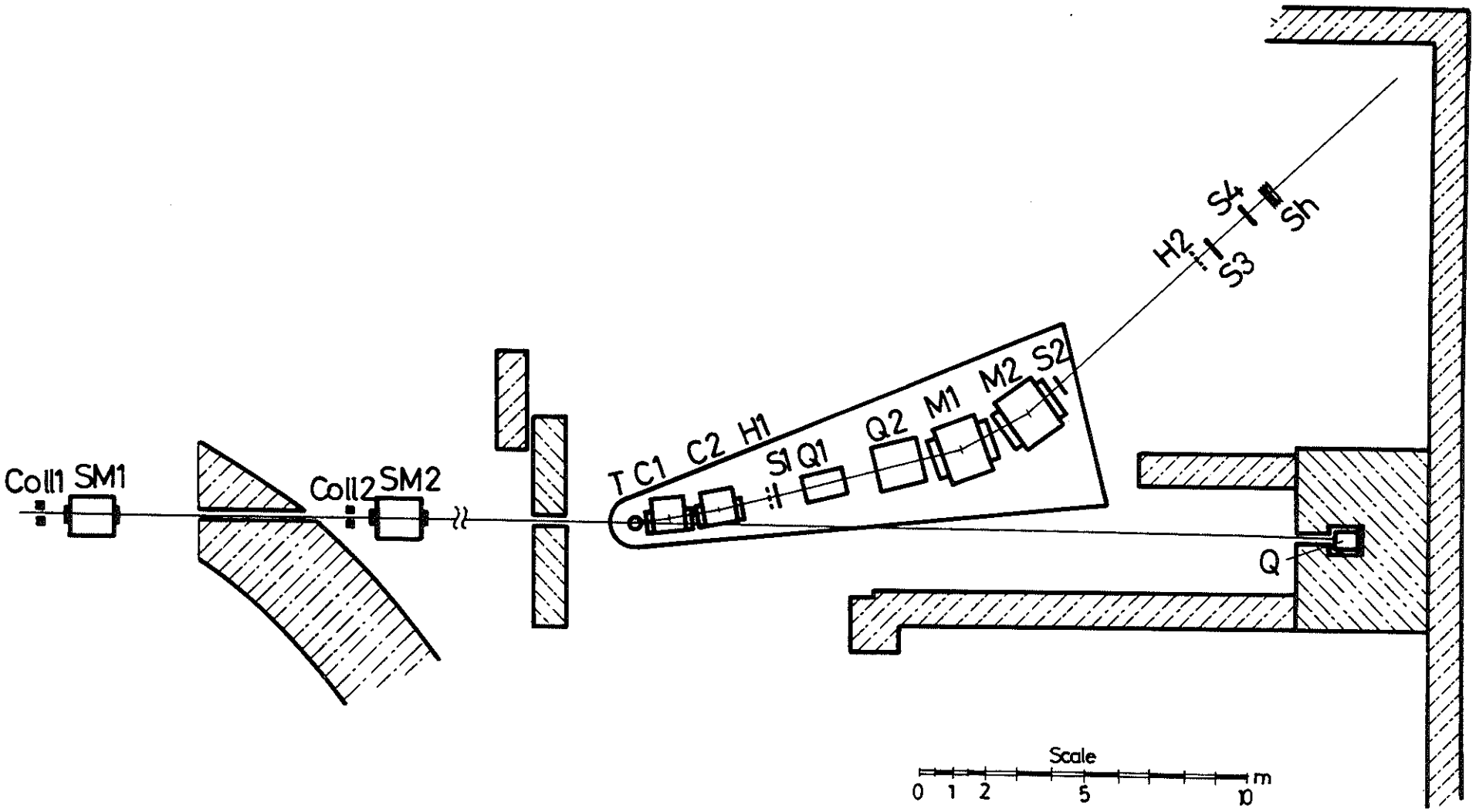
Coll1
SM1
Coll2
SM2
T
C1
C2
H1
S1
Q1
Q2
M1
M2
S2
H2
S3
S4
Sh
Q
Scale
0 1 2 5 10 m

Fig. 1

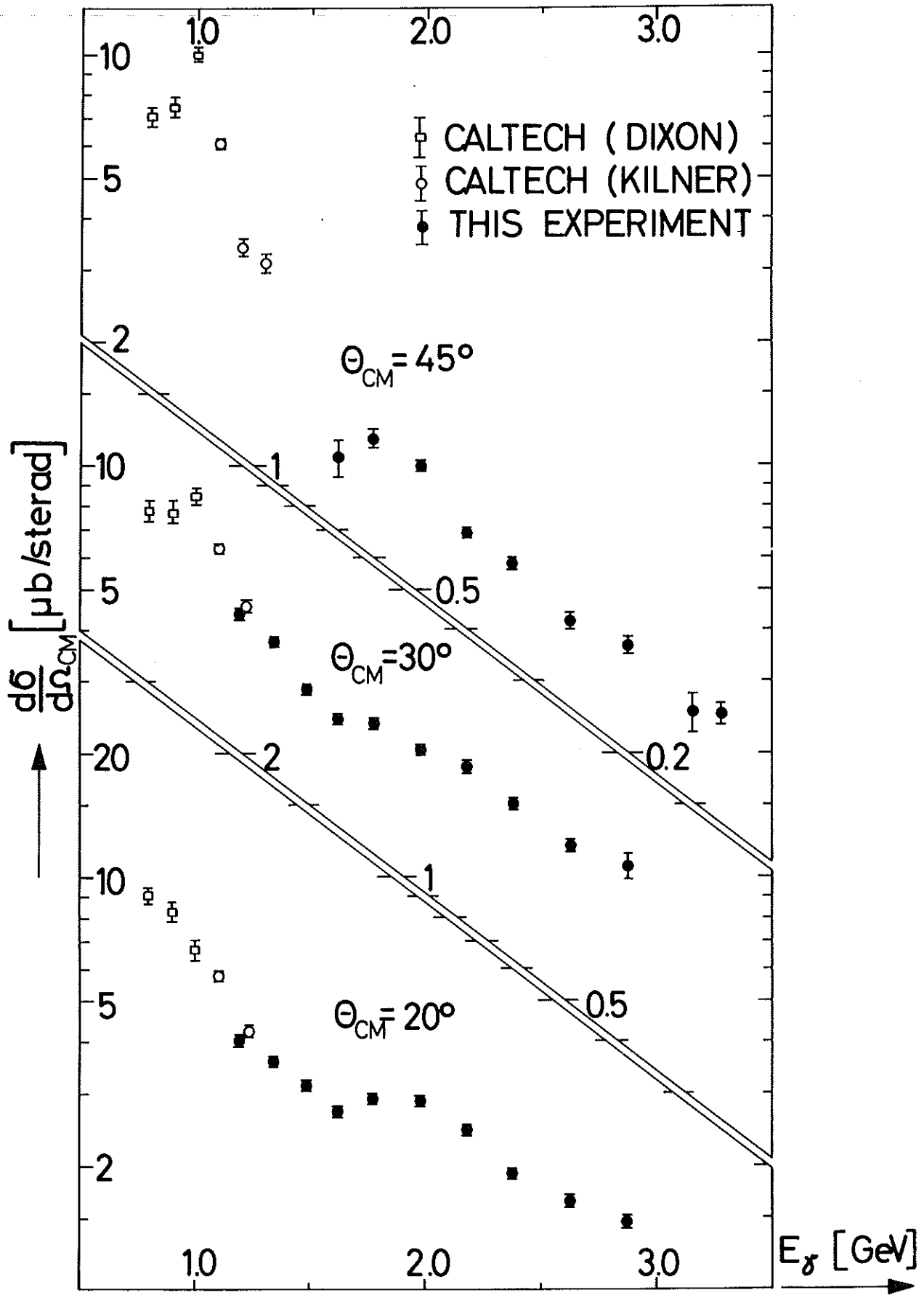
CALTECH (DIXON)
CALTECH (KILNER)
THIS EXPERIMENT
Θ_{CM}= 45°
Θ_{CM}=30°
Θ_{CM}= 20°
$\frac{d\sigma}{d\Omega_{CM}}$ [μb/sterad]
E_γ [GeV]
1.0
2.0
3.0
10
5
2
1
0.5
0.2
20

Fig. 2

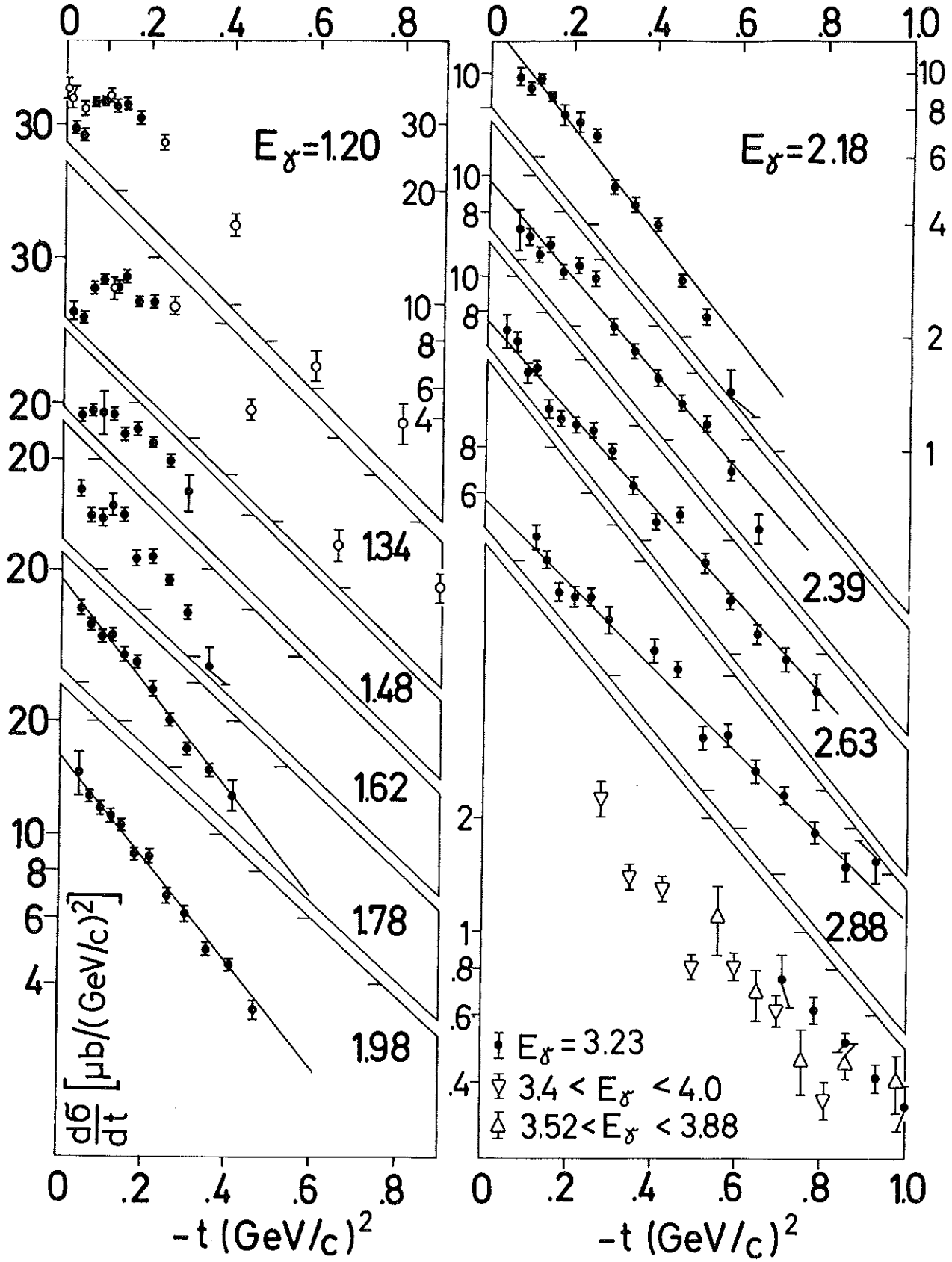
E_γ=1.20
E_γ=2.18
1.34
1.48
1.62
1.78
1.98
2.39
2.63
2.88
E_γ = 3.23
3.4 < E_γ < 4.0
3.52< E_γ < 3.88
$\frac{d\sigma}{dt}$ [μb/(GeV/c)^2]
-t (GeV/c)^2
-t (GeV/c)^2

Fig. 3